*Science in China Series G: Physics, Mechanics & Astronomy*



www.scichina.com
phys.scichina.com
www.springerlink.com

# Experimental investigation of particle velocity distributions in windblown sand movement

KANG LiQiang[1,2†], GUO LieJin[1] & LIU DaYou[2]

[1] State Key Laboratory of Multiphase Flow in Power Engineering, Xi'an Jiaotong University, Xi'an 710049, China;
[2] Division of Engineering Sciences, Institute of Mechanics, Chinese Academy of Sciences, Beijing 100190, China

**With the PDPA (Phase Doppler Particle Analyzer) measurement technology, the probability distributions of particle impact and lift-off velocities on bed surface and the particle velocity distributions at different heights are detected in a wind tunnel. The results show that the probability distribution of impact and lift-off velocities of sand grains can be expressed by a log-normal function, and that of impact and lift-off angles complies with an exponential function. The mean impact angle is between 28˚ and 39˚, and the mean lift-off angle ranges from 30˚ to 44˚. The mean lift-off velocity is 0.81—0.9 times the mean impact velocity. The proportion of backward-impacting particles is 0.05—0.11, and that of backward-entrained particles ranges from 0.04 to 0.13. The probability distribution of particle horizontal velocity at 4 mm height is positive skew, the horizontal velocity of particles at 20 mm height varies widely, and the variation of the particle horizontal velocity at 80 mm height is less than that at 20 mm height. The probability distribution of particle vertical velocity at different heights can be described as a normal function.**

windblown sand movement, probability distribution, particle velocity

## 1 Introduction

Windblown sand transport is prevalent in natural environments, such as arid deserts and sandy beaches. When the wind becomes strong enough, the sand particles on sand bed surface will be moved. The sand movement in windblown sand transport falls into three processes: creep, saltation and suspension. Saltation is the dominant mode of the blown sand movement, accounting for about 75% of the total sand flux[1]. The saltating grains transfer their momentum to the bed surface

Received October 31, 2007; accepted February 26, 2008
doi: 10.1007/s11433-008-0120-8
†Corresponding author (email: klq@sohu.com)
Supported by the National Natural Science Foundation of China (Grant No. 10532030) and the National Basic Research Program of China (Grant No. G2000048702)

through impact, so that more particles are emitted into the air. These emitted particles obtain more momentum from the air while moving in the wind, then descend under gravity and transfer their momentum to the bed surface through impact again. Therefore, saltation has been widely investigated in the study of windblown sand movement. Particle velocity distribution in a blowing sand cloud is a reflection of the saltation movement of many grains, and is also the main content of this paper.

Particle collision is intensive on the bed surface and can result in erosion. A large amount of saltating grains rebound after impacting the sand bed with different velocities and angles, or emit many other particles into the air. The grain-bed collision process determines the lift-off velocity distributions of particles, which further affect the particle trajectories and the sand flux. The lift-off velocity distribution of the saltating grains is also a bridge linking the microscopic and macroscopic aeolian research[2]. The research of Anderson and Haff[3] shows that the number of grains due to aerodynamic entrainment is rare at a steady state, and the saltating grains are mainly generated by particle impacts. Hence, it is important to study the motion state of saltating particles in the impact-entrainment process.

The particle velocity at different heights widely varies due to the saltation behavior. Dong et al.[4] found that the particle downwind velocity varies from –20.43 m/s to 20.56 m/s, and the particle vertical velocity variation ranges from –2.8 to 2.9 m/s, the probability distribution of the downwind sand velocity complies with a Gaussian function, while that of vertical velocity is a Lorentzian function for fine particles and is complex for coarse particles. Zou et al.[5] gave that the probability distribution of particle velocity is a Pearson VII distribution pattern. Greeley et al.[6] gave a result from the high-speed motion pictures that the velocity distributions of ascending and descending grains show a single peak.

Erosion by saltating particles is much stronger than that by clean wind, and sand velocity is a key factor in studying the vertical distribution of its kinetic energy, which determines the variation of abrasion intensity with height. From an impact energy consideration, Greeley and Iversen[7] obtained that the maximum wind erosion occurred on the parts close to the ground. While Sharp[8] found that the maximum abrasion occurred at about 0.1—0.15 m height above the ground. The wind tunnel experiments of Zou et al.[5] gave that the variation of kinetic energy of saltating sand grains with height accords with the Pulsepow law and is similar to the theoretical results of Anderson[9].

Reliable measurement technology is important for studying the particle velocity in blowing sand transport. Most observations use the high-speed photography to investigate the velocity and trajectory of an individual particle. However, the available number of particles from the high-speed photography is limited and insufficient for statistics, and it is difficult to deduce the sand velocity from the photographic images at the very low height (less than 5 mm) where the grains are too crowded.

Recently, the laser Doppler technology has been available to measure the particle velocity in the saltation layer[4,10]. The Phase Doppler Particle Analyzer (PDPA), which is a non-intrusive measurement, is suitable to measure the particle velocity at a fixed point. In this paper, the PDPA is used to measure the particle velocity in saltation, and further to study the probability characteristics of the velocity of the impacting and the lift-off grains and particle velocity distributions at different heights.

## 2 Experimental method

The experiment was performed in a sand wind tunnel at the State Key Laboratory of Multiphase Flow in Power Engineering, Xi'an Jiaotong University. The wind tunnel was a blow-type non-circulating wind tunnel. The working section of the wind tunnel was 12 m long with a cross-section which was 0.4 m wide and 0.6 m high. The roughness elements were placed in front of the working section in order to produce a thick boundary layer. The wind boundary layer thickness at the measurement position can reach about 0.16 m. The free-stream wind velocity in the wind tunnel can be changed continuously to 40 m/s.

The natural quartz sand was sieved into three size groups: 0.17—0.30, 0.30—0.36 and 0.36—0.44 mm. The layer of sand samples was about 4 m long, 0.4 m wide and 3—4 cm deep. According to the study of Dong et al.[11], the length of this sand layer can ensure a significant development of the saltating grains cloud.

The movement of blowing grains in saltation was measured by a Phase Doppler Particle Analyzer (PDPA). The free-stream wind velocity was measured by a hot wire anemometer at the start of the sand bed layer. The sketch of the experimental set-up in the working section of wind tunnel is shown in Figure 1.

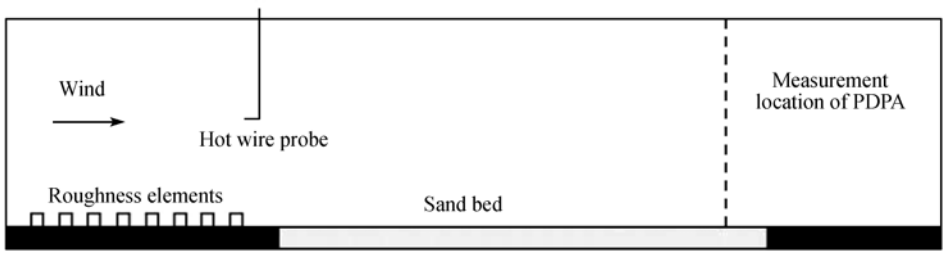


**Figure 1** Sketch of the experimental set-up in the working section of wind tunnel.

The PDPA is a non-intrusive measurement with a high accuracy. The 3-axis traverse system is used to precisely control the height of the velocity measurement points. The glass window of wind tunnel provides an optical access for the PDPA to produce the laser beams in the wind tunnel. The computer records the data of sand particle velocity.

The PDPA system is composed of laser, transmitting optics, receiving optics, signal processor and data collection. The physical principle of PDPA for velocity measurement is the Doppler effect. When the moving particle passes through the probe volume, the Doppler shift occurs, and the particle velocity in the direction vertical to the interference fringe is calculated by[12]

$$u_y = d_f f_D, \tag{1}$$

where $f_D$ is the Doppler frequency, and $d_f$ is the fringe spacing which goes as follows:

$$d_f = \frac{\lambda}{2\sin\beta}, \tag{2}$$

where $\lambda$ is the laser wavelength, and $\beta$ is half angle between beams.

The setting parameters of PDPA in the experiments are listed in Table 1.

In the wind tunnel experiments of the windblown sand movement, the wind velocity profile should be similar between model and prototype.

**Table 1** The setting parameters of PDPA

| Item | Specification |
|---|---|
| Transmitting lens focal length | 600 mm |
| Wavelength | 514.5 nm (green) |
| | 488 nm (blue) |
| Beam separation | 25 mm (green) |
| | 50 mm (blue) |
| Laser beam diameter | 1.8 mm (green) |
| | 1.8 mm (blue) |
| Fringe spacing | 12.35 μm (green) |
| | 5.86 μm (blue) |
| Probe volume length | 10.484 mm (green) |
| | 4.975 mm (blue) |
| Waist diameter | 0.218 mm (green) |
| | 0.207 mm (blue) |

The wind velocity profile in the clear wind and above the saltation layer follows the logarithmic law. In the saltation layer, the wind velocity profile does not perfectly obey the logarithmic function due to the presence of saltating grains, especially in the near-bed layer. However, if the wind flow above the saltation layer is similar, the wind flow within the saltation layer will be similar.

The logarithmic wind velocity profile can be expressed as

$$\frac{u}{u_*} = \frac{1}{k}\ln\frac{z}{z_0}, \tag{3}$$

where $u$ is wind velocity at the height $z$, $k$ is von Karman's constant, $u_*$ is the friction velocity, and $z_0$ is the roughness length.

In eq. (3), $u/u_*$ and $z/z_0$ can be considered as non-dimensional wind velocity and non-dimensional height, respectively. From eq. (3), if the wind velocity profile follows the logarithmic law in the wind tunnel, the wind tunnel tests will be similar to the actual blowing sand movement.

## 3 Results and analysis

### 3.1 Probability distribution of impact velocity and angle of saltating particles on bed surface

In the impact-entrainment process above the sand bed surface, if the vertical velocity of a particle is downward, the particle will be descending and is considered as the impacting particle, otherwise it is the lift-off particle. The particle impact velocity is the resultant velocity of the horizontal and vertical velocities of impacting particles. The particle impact angle is the angle between the particle impact velocity and the free-stream wind direction. The particle lift-off velocity is the resultant velocity of the horizontal and vertical velocities of the lift-off particles. The particle lift-off angle is the angle between the particle lift-off velocity and the free-stream wind direction.

The probability distribution of the particle impact velocity is shown in Figure 2. $d_p$ is the sand diameter. $u_{f0}$ is the free-stream wind velocity. It can be seen from Figure 2 that the distributions of the particle impact velocity have a typical peak.

The probability distribution of the particle impact velocity can be described by a log-normal function which goes as follows:

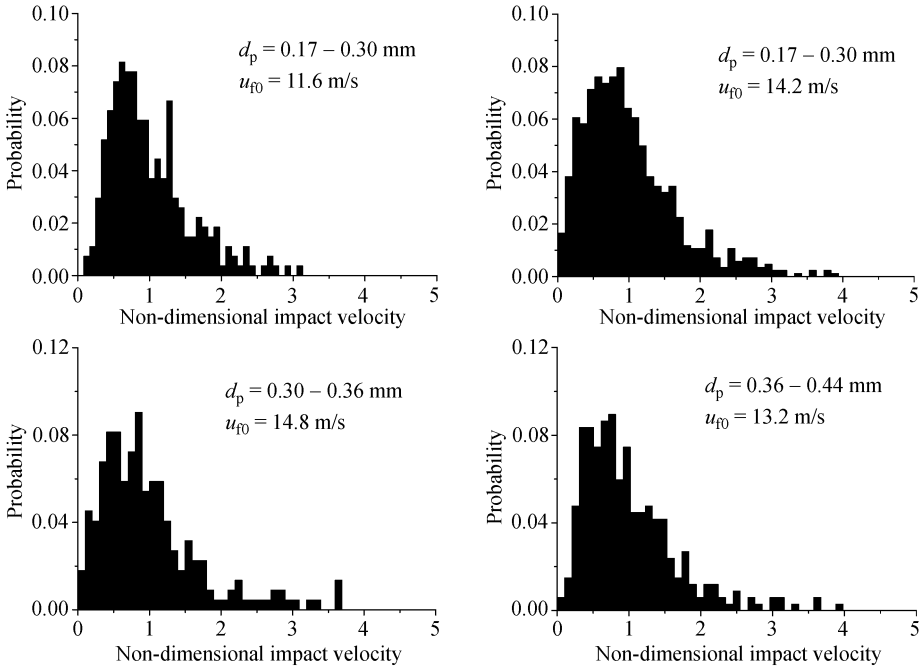


**Figure 2** Probability distribution of particle impact velocity.

$$P(u_I^*) = \frac{A}{\sqrt{2\pi}Bu_I^*}\exp\left(-\frac{(\ln u_I^* - \ln C)^2}{2B^2}\right), \tag{4}$$

where $P$ is the probability, $u_I^*$ is the non-dimensional particle impact velocity, $u_I^* = u_I / U_I$. $u_I$ and $U_I$ are the particle impact velocity and its average (m/s), respectively. $A$, $B$ and $C$ are constants.

Table 2 lists the curve-fit parameters of the particle impact velocity distribution. $R^2$ is the correlation coefficient. It can be seen that the correlation between curve-fit function and experimental data is better. The correlation coefficients of the most fitting curves are more than 0.9.

**Table 2** Fitting parameters of the particle impact velocity distribution

| Sand diameter (mm) | Free-stream wind velocity (m/s) | $A$ | $B$ | $C$ | $R^2$ |
|---|---|---|---|---|---|
| 0.17−0.30 | 10.9 | 0.087 | 0.578 | 0.819 | 0.86 |
| | 11.6 | 0.083 | 0.581 | 0.879 | 0.94 |
| | 14.2 | 0.109 | 0.758 | 0.934 | 0.94 |
| 0.30−0.36 | 11.1 | 0.114 | 0.624 | 0.802 | 0.98 |
| | 14.8 | 0.102 | 0.744 | 0.879 | 0.89 |
| 0.36−0.44 | 12.3 | 0.123 | 0.636 | 0.872 | 0.94 |
| | 13.2 | 0.105 | 0.684 | 0.866 | 0.96 |
| | 15.8 | 0.104 | 0.707 | 0.864 | 0.90 |

Figure 3 denotes the probability distribution of the particle impact angle. It can be seen from Figure 3 that the particle impact angle distribution is similar to an exponential distribution, which can be described by the following exponential function:

$$P(\alpha_I) = \frac{1}{A}\exp\left(-\frac{\alpha_I}{B}\right), \tag{5}$$

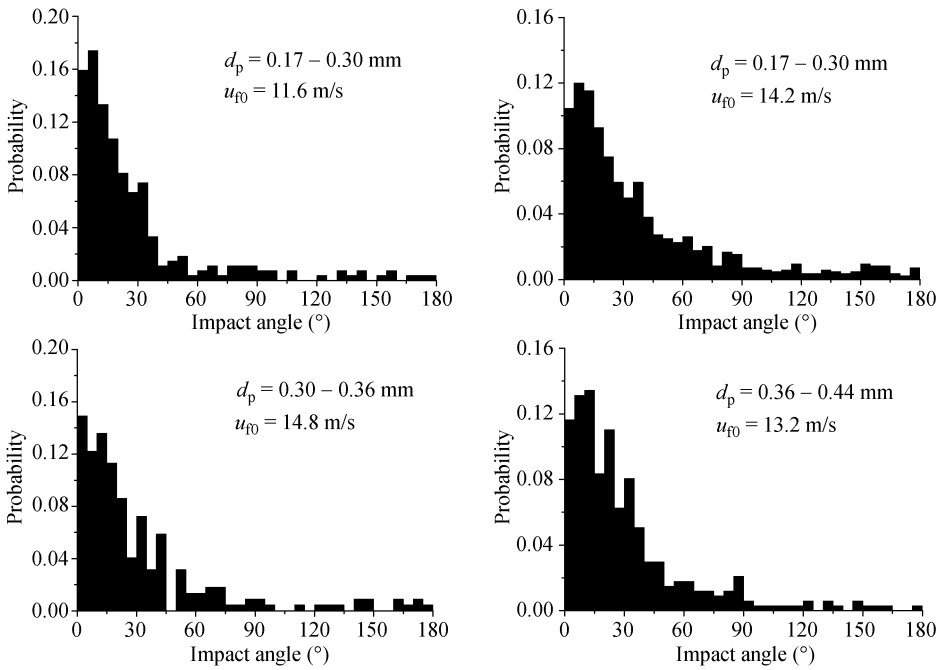


**Figure 3** Probability distribution of particle impact angle.

where $P$ is the probability, $\alpha_1$ is the particle impact angle (°), $A$ and $B$ are constants.

Table 3 shows the curve-fit parameters of probability distribution of the particle impact angle. $R^2$ is the correlation coefficient. Except one fitting curve, the correlation coefficients of the other fitting curves are more than 0.9.

**Table 3** Fitting parameters of probability distribution of the particle impact angle

| Sand diameter (mm) | Free-stream wind velocity (m/s) | $A$ | $B$ | $R^2$ |
|---|---|---|---|---|
| 0.17—0.30 | 10.9 | 5.0 | 24.5 | 0.88 |
| | 11.6 | 4.8 | 23.7 | 0.96 |
| | 14.2 | 7.4 | 36.3 | 0.96 |
| 0.30—0.36 | 11.1 | 7.2 | 35.2 | 0.93 |
| | 14.8 | 5.7 | 28.0 | 0.93 |
| 0.36—0.44 | 12.3 | 8.0 | 41.0 | 0.91 |
| | 13.2 | 6.3 | 32.5 | 0.93 |
| | 15.8 | 6.2 | 30.7 | 0.97 |

It is also seen from Figure 3 that the impact angles of some impact particles are more than 90°, that is to say, these particles impact the sand bed in the opposite direction to the wind. These backward-impacting particles are mainly related to the mid-air collisions which are important for the generation of the backward grains. Further analysis shows that the proportion of the backward-impacting particles is 0.05—0.11, while Dong et al.[13] reported that the proportion of the backward-impacting particles was 0.11—0.43.

In this paper, the measured particle mean impact angle ranges from 28° to 39°, which is larger than some reported results[1,14–17]: 10°—16°, 6°—12°, 13.9°, 9.6°—12.7° and 11°—14°, but smaller than the result (40°—78°) of Dong et al.[13].

The difference of the results between this paper and the high-speed photography probably attributes to the difference of the particle sample. With the high-speed photography, it is still difficult to see what happens when a saltating particle impacts the sand bed surface. Hence, Nalpanis et al.[17] extrapolated each measured particle trajectory to the bed surface and then collected trajectory statistics, but some trajectories of the low-energy particles close to the bed surface will be omitted because these trajectories cannot be identified on the high-speed photos.

In the wind tunnel experiments of Dong et al.[13], the free-stream wind velocity is between 8 m/s and 18 m/s, the cross-section in the working section of wind tunnel is 0.6 m high and 1 m wide, the sand layer is 2.5 m long, and the diameter of sand particles ranges from 0.1 mm to 0.6 mm. In the present experiments, the free-stream wind velocity is 10.9—15.8 m/s, the diameter of the sand particles is 0.17—0.44 mm, and these conditions are within the experimental conditions of Dong et al.[13]. The sand layer of this paper is 4 m long, which is more than that of Dong et al.[13] and can ensure a significant development of the saltating grains cloud. Therefore, the results of this paper are more reliable.

### 3.2 Probability distribution of lift-off velocity and angle of saltating particles on bed surface

The probability distribution of the particle lift-off velocity is shown in Figure 4. It can be seen that the distributions of the particle lift-off velocity are similar to those of the particle impact velocity, and both of them have a typical peak.

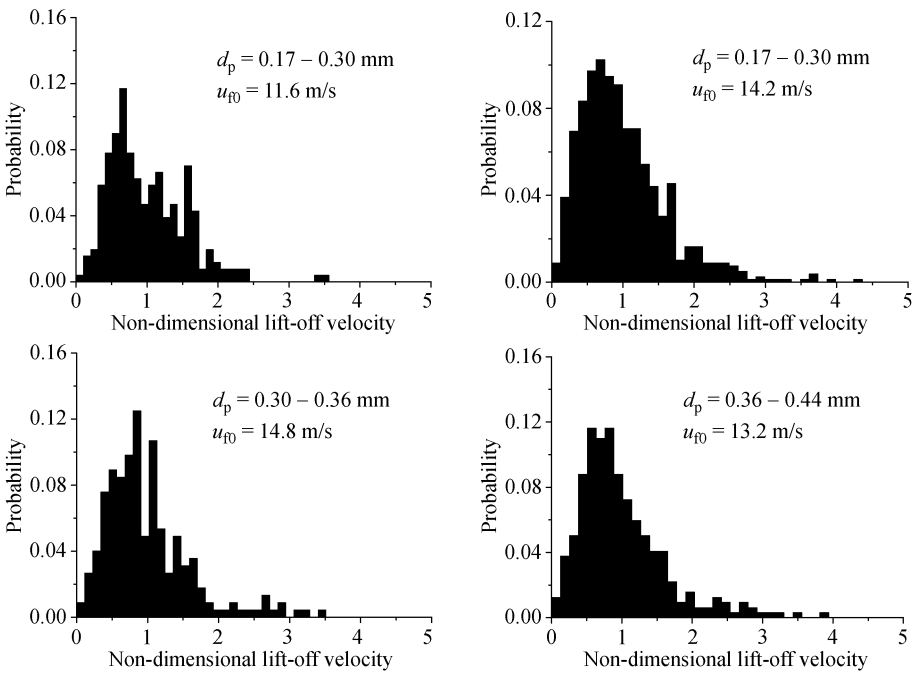


**Figure 4** Probability distribution of particle lift-off velocity.

In the experiments, the particle lift-off velocity ranges from 0 to 3 m/s and the particle impact velocity varies from 0 to 3.75 m/s, but the proportion of high energy particles is low.

The probability distribution of the particle lift-off velocity can be described by the following log-normal function:

$$P(u_{\mathrm{L}}^{*}) = \frac{A}{\sqrt{2\pi}Bu_{\mathrm{L}}^{*}} \exp\left( -\frac{(\ln u_{\mathrm{L}}^{*} - \ln C)^2}{2B^2} \right), \tag{6}$$

where $P$ is the probability, $u_{\mathrm{L}}^{*}$ is the non-dimensional particle lift-off velocity, $u_{\mathrm{L}}^{*} = u_{\mathrm{L}} / U_{\mathrm{L}}$. $u_{\mathrm{L}}$ and $U_{\mathrm{L}}$ are the particle lift-off velocity and its average (m/s), respectively. $A$, $B$ and $C$ are constants.

Table 4 lists the curve-fit parameters of the particle lift-off velocity distribution. The correlation coefficients of most fitting curves are more than 0.9, and the correlation between curve-fit function and experimental data is better.

**Table 4** Fitting parameters of the particle lift-off velocity distribution

| Sand diameter (mm) | Free-stream wind velocity (m/s) | $A$ | $B$ | $C$ | $R^2$ |
|---|---|---|---|---|---|
| 0.17—0.30 | 10.9 | 0.102 | 0.656 | 0.88 | 0.91 |
| | 11.6 | 0.104 | 0.61 | 0.912 | 0.88 |
| | 14.2 | 0.129 | 0.668 | 0.919 | 0.97 |
| 0.30—0.36 | 11.1 | 0.135 | 0.707 | 0.90 | 0.92 |
| | 14.8 | 0.113 | 0.579 | 0.895 | 0.88 |
| 0.36—0.44 | 12.3 | 0.139 | 0.666 | 0.829 | 0.97 |
| | 13.2 | 0.125 | 0.577 | 0.883 | 0.97 |
| | 15.8 | 0.118 | 0.6 | 0.93 | 0.90 |

Figure 5 denotes the probability distribution of the particle lift-off angle. It can be seen from Figure 5 that the particle lift-off angle distribution is similar to an exponential distribution. The variation of the particle lift-off angle is wide. The angle of some lift-off particles is larger than 90°, hence, the particle collisions are intensive near the bed surface.

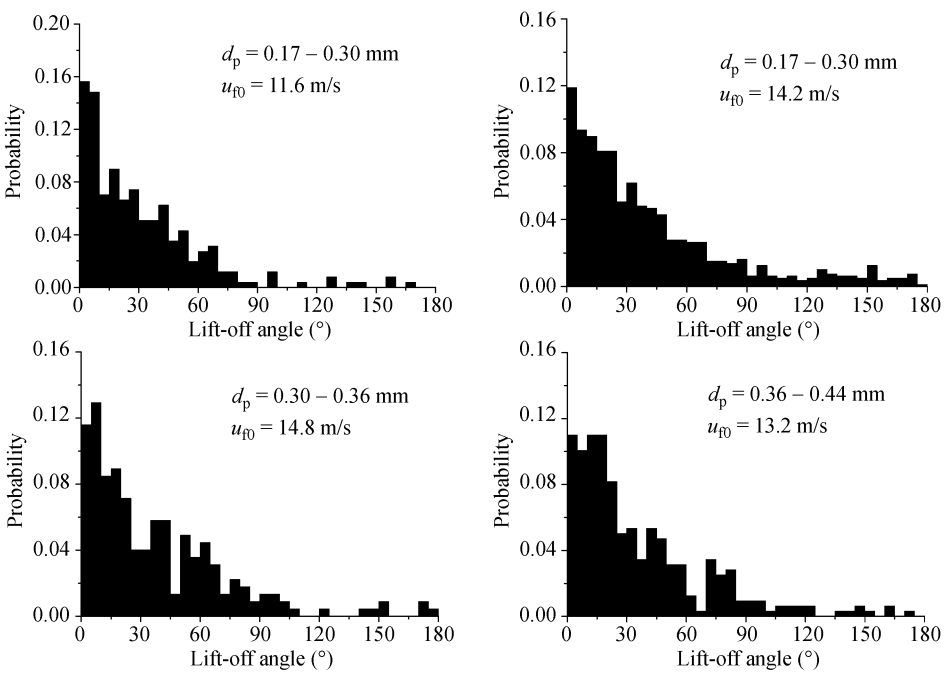


**Figure 5** Probability distribution of particle lift-off angle.

Bagnold[1], Chepil[14] and Owen[18] suggested that many particles rose almost vertically from the sand bed. The particle mean lift-off angle of this paper is 30°—44°, similar to the reported result of Nalpanis et al.[17] (34°—41°), but less than the result of Dong et al.[13] (39°—94°). Probably the reasons are that the sand sample and the experimental conditions are different.

The probability distribution of the particle lift-off angle can be described by the following exponential function:

$$P(\alpha_{\mathrm{L}}) = \frac{1}{A}\exp\left(-\frac{\alpha_{\mathrm{L}}}{B}\right), \tag{7}$$

where $P$ is the probability, $\alpha_{\mathrm{L}}$ is the particle impact angle (°), $A$ and $B$ are constants.

Table 5 shows the curve-fit parameters of probability distribution of the particle lift-off angle. The correlation between curve-fit function and experimental data is better.

**Table 5** Fitting parameters of probability distribution of the particle lift-off angle

| Sand diameter (mm) | Free-stream wind velocity (m/s) | $A$ | $B$ | $R^2$ |
|---|---|---|---|---|
| 0.17—0.30 | 10.9 | 7.8 | 39.1 | 0.84 |
| | 11.6 | 6.2 | 31.1 | 0.94 |
| | 14.2 | 8.2 | 40.6 | 0.98 |
| 0.30—0.36 | 11.1 | 8.0 | 40.1 | 0.92 |
| | 14.8 | 7.7 | 38.7 | 0.92 |
| 0.36—0.44 | 12.3 | 8.8 | 44.3 | 0.95 |
| | 13.2 | 7.6 | 38.8 | 0.93 |
| | 15.8 | 6.8 | 34.2 | 0.93 |

Some wind tunnel experimental results from the high-speed photography show that the probability density distributions of the lift-off velocity and angle are similar to a log-normal distribution or a gamma distribution[15—17], but Anderson and Hallet[19] suggested using the exponential distribution because available wind tunnel observations may be biased towards the more easily observed high-energy trajectories. The wind tunnel experimental results of Dong et al.[13] show that the velocity distribution of the impact and entrained particles is described by the Weibull function, while the probability distribution of the impact and lift-off angles cannot be expressed by a simple function.

In this paper, the probability distribution of the impact and lift-off velocities of sand grains can be expressed by a log-normal function, and that of the impact and lift-off angles complies with an exponential function. The present work supplies an experimental reference for the study of particle velocity distributions on the bed surface.

### 3.3 Particle impact-entrainment relationship

The relationship between the particle mean impact and lift-off velocities is shown in Figure 6. If the particle mean impact velocity is higher, the particle mean lift-off velocity will be higher, and *vice versa*. This is consistent with the report of Dong et al.[13].

The relationship between the particle mean impact and lift-off velocities can be expressed as

$$U_{\mathrm{L}} = 0.14 + 0.718U_{\mathrm{I}}, \quad R^2 = 0.93, \tag{8}$$

where $U_{\mathrm{L}}$ and $U_{\mathrm{I}}$ are the particle mean lift-off and impact velocities, respectively.

It is also seen from Figure 6 that the particle mean lift-off velocity is less than the particle mean impact velocity, which is reasonable because there is an energy loss during the particle collisions.

According to the present experiments, the particle mean lift-off velocity is 0.81—0.9 times the mean impact velocity, or the particle mean impact velocity is 1.11—1.24 times the mean lift-off velocity. The ratio of the particle mean impact velocity to the mean lift-off velocity is reported by some references as 1.6—2[17], 2.3[15], 1.6[16], while Dong et al.[13] reported the wide ratio of the particle mean lift-off velocity to the mean impact velocity is 0.48—1.17.

Figure 7 denotes the relationship of the particle mean impact and lift-off angles. The particle mean lift-off angle is larger than the mean impact angle. This is obvious because the particle vertical velocity descends due to air drag force and the particle horizontal velocity increases due to the wind velocity. The particle mean lift-off angle generally increases with the increase of mean impact angle.

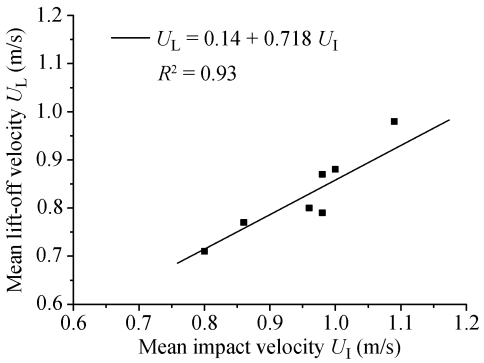


**Figure 6** Relationship of particle mean impact and lift-off velocities.

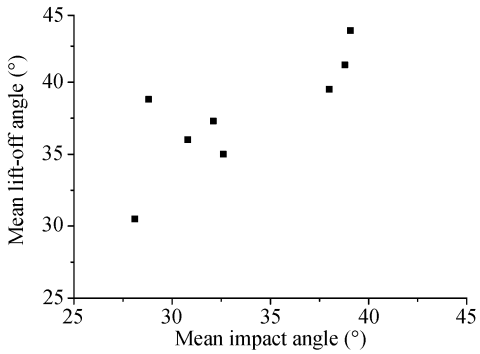


**Figure 7** Relationship of particle mean impact and lift-off angles.

Table 6 shows the measured number of the impact and lift-off particles. It can be seen that the number ratio of the lift-off particles to the impact particles is from 0.94 to 1.12. In the experiments, some sand bed is in the net loss of the surface sand, and some lies in the sedimentary state.

Table 6 also lists the number of the backward-impacting and backward-entrained particles. The horizontal velocity of these particles is opposite to the wind direction. The proportion of the backward-impacting particles is 0.05—0.11, and that of the backward-entrained particles ranges from 0.04 to 0.13.

The backward proportion of impact particles is related better to that of the lift-off particles, as shown in Figure 8. If the number of the backward-impacting particles increases, that of the backward-entrained particles will increase in general. Regressive analysis shows that the backward

**Table 6** The number of impact and lift-off particles

| Sand diameter (mm) | Free-stream wind velocity (m/s) | $N_I$ | $N_{IB}$ | $N_{IB}/N_I$ | $N_L$ | $N_{LB}$ | $N_{LB}/N_L$ | $N_L/N_I$ |
|---|---|---|---|---|---|---|---|---|
| 0.17—0.30 | 10.9 | 195 | 14 | 0.07 | 218 | 20 | 0.09 | 1.12 |
| | 11.6 | 270 | 18 | 0.07 | 256 | 11 | 0.04 | 0.95 |
| | 14.2 | 841 | 89 | 0.11 | 791 | 92 | 0.12 | 0.94 |
| 0.30—0.36 | 11.1 | 320 | 30 | 0.09 | 323 | 34 | 0.11 | 1.01 |
| | 14.8 | 221 | 17 | 0.08 | 224 | 17 | 0.08 | 1.01 |
| 0.36—0.44 | 12.3 | 533 | 60 | 0.11 | 500 | 67 | 0.13 | 0.94 |
| | 13.2 | 335 | 18 | 0.05 | 318 | 23 | 0.07 | 0.95 |
| | 15.8 | 263 | 19 | 0.07 | 269 | 20 | 0.07 | 1.02 |

$N_I$ is the total number of impact particles, $N_{IB}$ is the number of backward-impacting particles, $N_L$ is the total number of lift-off particles, and $N_{LB}$ is the number of backward-entrained particles.

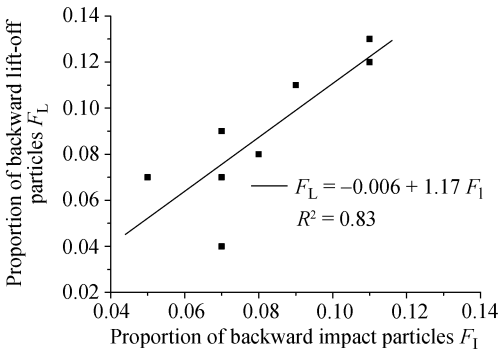


**Figure 8** Proportion relationship of backward impact and lift-off particles.

proportion of impact particles is linear to that of the lift-off particles:

$$F_L = -0.006 + 1.17F_I, \quad R^2 = 0.82, \tag{9}$$

where $F_L$ and $F_I$ are the backward proportion of lift-off and impact particles, respectively.

### 3.4 Particle velocity distributions at different heights

The particle velocity distribution at different heights is a reflection of the saltation movement of many sand grains.

In the following, the probability distributions of particle horizontal and vertical velocities are analyzed at three different heights. Three selected heights are in the different parts of the saltation layer, i.e., 4 mm, 20 mm and 80 mm.

Figure 9 is the probability distribution of the particle horizontal velocity at different heights. In Figure 9, $z$ is the height. $u_p^*$ is the non-dimensional particle horizontal velocity, $u_p^* = u_p / \overline{u}_p$, where $u_p$ and $\overline{u}_p$ are the particle horizontal velocity and its mean, respectively. It can be seen that the shapes of these histograms have a typical peak. At 4 mm height, the probability distributions of the particle horizontal velocity are asymmetrical and show a positive skewness. The horizontal velocity of many particles focuses on about 1 m/s, while the particles with higher horizontal velocity are few. Probably the reason of this is that during the splash process, only a single particle may receive a large part of the momentum of the impact grain, while more grains will receive little momentum and thus make low and short jumps. It can be also seen from Figure 9 that at 4 mm height, there are some backward-movement particles due to the intensive particle collisions in the lower part of the saltation layer.

At the 20 mm height, the variation of particle horizontal velocity is large, and the particle collisions become weak. There are not only low-energy saltating particles from the bed surface, but also high-energy saltating particles accelerated by wind.

At 80 mm height in the upper part of the saltation layer, the particle collisions are very weak. Only the high-energy saltating particles can reach this height.

Compared with the 80 mm height, if a saltating particle ascends from the 20 mm height, this particle will take more time to descend to the same height, and the horizontal velocity variation of this particle is large. Hence, the changed range of the particle horizontal velocity at 80 mm height is less than that at 20 mm height.

Figure 10 denotes the particle vertical velocity distributions at different heights. $v_p^*$ is the non-dimensional particle vertical velocity, $v_p^* = v_p / \overline{u}_p$, where $v_p$ is the particle vertical velocity.

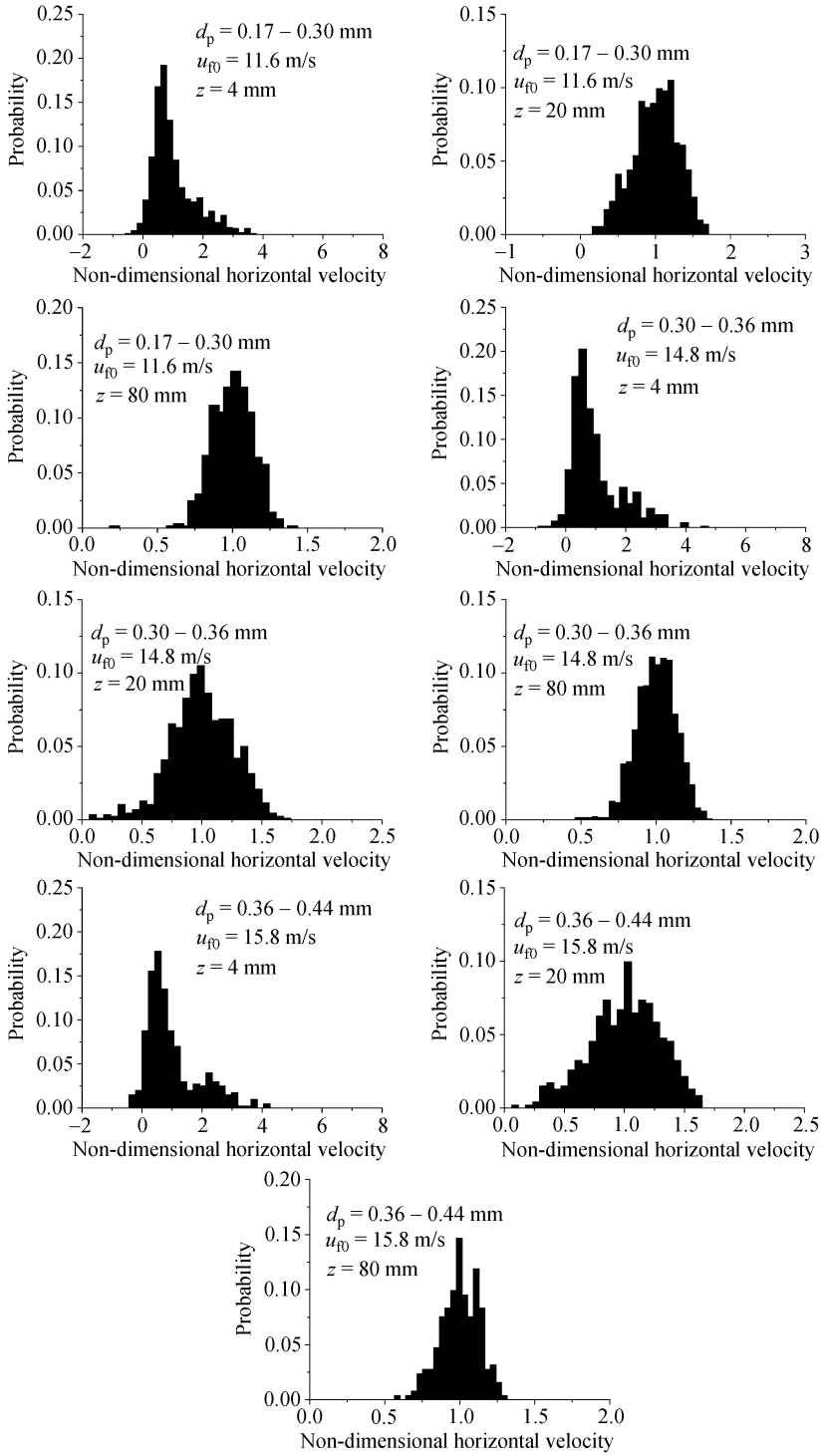


**Figure 9** Probability distribution of particle horizontal velocity.

It can be seen that the particle vertical velocity distributions at different heights are similar to the normal distribution, and can be expressed as

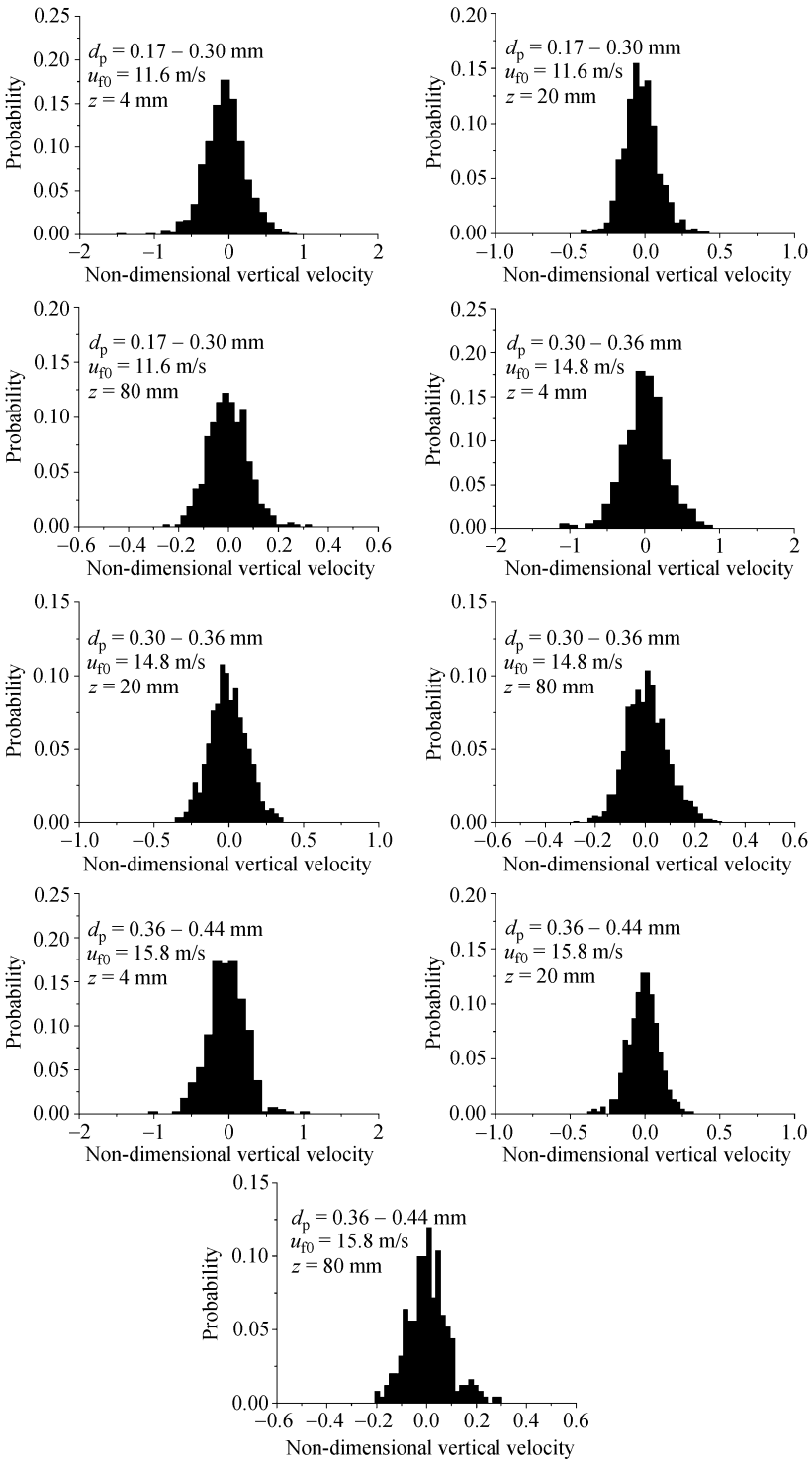


**Figure 10** Probability distribution of particle vertical velocity.

$$P(v_p^*) = \frac{A}{\sqrt{2\pi}B}\exp\left(-\frac{(v_p^* - C)^2}{2B^2}\right), \tag{10}$$

where $P$ is the probability, $A$, $B$ and $C$ are constants.

The fitting parameters of the particle vertical velocity distribution are shown in Table 7. The correlation between curve-fit function and experimental data is better. Except one fitting curve, the correlation coefficients of the other fitting curves are more than 0.97.

**Table 7** Fitting parameters of particle vertical velocity distribution

| Sand diameter (mm) | Free-stream wind velocity (m/s) | Height (mm) | $A$ | $B$ | $C$ | $R^2$ |
|---|---|---|---|---|---|---|
| 0.17—0.30 | 11.6 | 4 | 0.096 | 0.231 | –0.051 | 0.99 |
| | | 20 | 0.038 | 0.103 | –0.033 | 0.98 |
| | | 80 | 0.024 | 0.078 | –0.004 | 0.98 |
| 0.30—0.36 | 14.8 | 4 | 0.109 | 0.252 | 0.007 | 0.98 |
| | | 20 | 0.03 | 0.122 | –0.009 | 0.97 |
| | | 80 | 0.019 | 0.079 | 0.001 | 0.97 |
| 0.36—0.44 | 15.8 | 4 | 0.105 | 0.231 | –0.023 | 0.98 |
| | | 20 | 0.029 | 0.094 | –0.008 | 0.98 |
| | | 80 | 0.018 | 0.072 | 0.003 | 0.91 |

It is also found in the experiments that the particle vertical velocity generally changes between –2 m/s and 2 m/s, and this is consistent with the report of Dong et al.[4], who gave the particle vertical velocity varies from −2.8 m/s to 2.9 m/s.

## 4 Conclusions

The probability distributions of the particle impact and lift-off velocities on bed surface and the particle velocity distributions at different heights in windblown sand movement are analyzed in detail. The results show that the probability distribution of the impact and lift-off velocities of the sand grains can be expressed by a log-normal function, and that of the impact and lift-off angles complies with an exponential function.

The particle impact parameters are related to the lift-off parameters. The mean lift-off velocity of the sand particles is less than the mean impact velocity. If the particle mean impact velocity is large, the mean lift-off velocity will be also large. The particle mean lift-off angle is larger than the mean impact angle, and generally increases with the increase of mean impact angle.

The backward proportion of the impact particles is also related to that of lift-off particles. If the number of backward-impacting particles increases, that of backward-entrained particles will increase in general. The particle collision is important to these backward-movement particles.

The probability distribution of the particle horizontal velocity is different at different heights. The distribution of the particle horizontal velocity at 4 mm height is positive skew, the horizontal velocity of particles at 20 mm height varies widely, and the variation of the particle horizontal velocity at 80 mm height is less than that at 20 mm height. The probability distribution of particle vertical velocity at different heights can be described as a normal function.

The present results supply an experimental reference for the study of particle velocity distributions and also provide the experimental data for the study of the theoretical research in windblown sand movement.

1 Bagnold R A. The Physics of Blown Sand and Desert Dunes. London: Methuen, 1941

2 Cheng H, Zou X Y, Zhang C L. Probability distribution functions for the initial liftoff velocities of saltating sand grains in air.

J Geophys Res-Atmospheres, 2006, 111: D22205[DOI]
3 Anderson R S, Haff P K. Wind modification and bed response during saltation of sand in air. Acta Mech, 1991, (suppl.1): 21－51
4 Dong Z B, Liu X P, Wang X M, et al. Experimental investigation of the velocity of a sand cloud blowing over a sandy surface. Earth Sur Proc Land, 2004, 29: 343－358[DOI]
5 Zou X Y, Wang Z L, Hao Q Z, et al. The distribution of velocity and energy of saltating sand grains in a wind tunnel. Geomorphology, 2001, 36: 155－165[DOI]
6 Greeley R, Blumberg D G, Williams S H. Field measurements of the flux and speed of wind-blown sand. Sedimentology, 1996, 43: 41－52[DOI]
7 Greeley R, Iversen J D. Wind as A Geological Process on Earth, Mars, Venus and Titan. Cambridge: Cambridge Univ. Press, 1985
8 Sharp R P. Wind-driven sand in Coachella Valley, California. Geo Soc Am Bull, 1964, 75: 785－804[DOI]
9 Anderson R S. Erosion profiles due to particle entrained by wind: Application of an eolian sediment-transport model. Geol Soc Am Bull, 1986, 97: 1270－1278[DOI]
10 Dong Z B, Wang H T, Liu X P, et al. Velocity profile of a sand cloud blowing over a gravel surface. Geomorphology, 2002, 45: 277－289[DOI]
11 Dong Z B, Wang H T, Liu X P, et al. The blown sand flux over a sandy surface: A wind tunnel investigation on the fetch effect. Geomorphology, 2004, 57: 117－127[DOI]
12 Crowe C T, Sommerfeld M, Tsuji Y. Multiphase Flows with Droplets and Particles. Boca Raton: CRC Press, 1998
13 Dong Z B, Liu X P, Li F, et al. Impact-entrainment relationship in a saltating cloud. Earth Sur Proc Land, 2002, 27: 641－658 [DOI]
14 Chepil W S. Dynamics of wind erosion (I): Nature of movement by wind. Soil Sci, 1945, 60: 305－320
15 White B R, Schulz J C. Magnus effect on saltation. J Fluid Mech, 1977, 81: 497－512[DOI]
16 Willetts B B, Rice M A. Intersaltating collisions. In: Barndorff-Nielsen O E, et al., eds. Proceedings of International Workshop on the Physics of Blown Sand. Denmark: University of Aarhus, 1985. 83－100
17 Nalpanis P, Hunt J C R, Barrett C F. Saltating particles over flat beds. J Fluid Mech, 1993, 251: 661－685[DOI]
18 Owen P R. Saltation of uniform grains in air. J Fluid Mech, 1964, 20(2): 225－242[DOI]
19 Anderson R S, Hallet B. Sediment transport by wind: Toward a general model. Geol Soc Am Bull, 1986, 97: 523－535 [DOI]